

# Correlations in the T Cell Response to Altered Peptide Ligands

Jeong-Man Park<sup>1,2</sup> and Michael W. Deem<sup>1</sup>

<sup>1</sup>*Department of Physics & Astronomy and Department of Bioengineering  
Rice University, Houston, TX 77005-1892*

<sup>2</sup>*Department of Physics  
The Catholic University of Korea, Puchon 420-743, Korea*

---

## Abstract

The vertebrate immune system is a wonder of modern evolution. Occasionally, however, correlations within the immune system lead to inappropriate recruitment of preexisting T cells against novel viral diseases. We present a random energy theory for the correlations in the naive and memory T cell immune responses. The non-linear susceptibility of the random energy model to structural changes captures the correlations in the immune response to mutated antigens. We show how the sequence-level diversity of the T cell repertoire drives the dynamics of the immune response against mutated viral antigens.

*Key words:* random energy model, immune system, altered peptide ligands

*PACS:* 87.23.Kg, 87.10.+e, 87.15.Aa, 87.17.-d

---

## 1 Introduction

In this work, we develop a random energy model that allows us to address limitations in the cellular immune system response to mutable viral diseases. We focus on the T cell response, with an emphasis on cytotoxic lymphocyte (CTL) T cells, which bind the peptide-major histocompatibility class I (MHC I) complex [1]. These T cells eradicate other infected cells through an interaction mediated by the binding of the T cell receptor (TCR) to antigenic peptides derived from the infectious disease. The finite number of different T cells within an individual and the existence of immune system memory makes the immune system response to mutating viral diseases nontrivial. We seek to understand how the T cell receptor repertoire changes within the immune system in response to repeated exposure to evolving viral diseases.

The immune system has a mechanism for selecting among the many possible TCRs those that best bind to the antigenic peptides. TCRs are constructed from modular elements, and each individual has an approximate diversity of  $2.5 \times 10^7$  different receptors [2]. TCRs undergo rounds of selection for increased affinity [3]. TCRs do not undergo any further mutation during the immune response. Those TCRs that are stochastically selected in the primary response to a disease become memory cells [4]. While many details affect the T cell selection process [5,6], selection for increased affinity is thought to be a dominant factor [7].

Several limitations of the cellular immune system have been reported that stem from the fact that a single T cell receptor may bind multiple antigenic peptides. This cross-reactivity is studied in quantitative molecular experiments through the use of altered peptide ligands (APLs), peptides that differ from the native ligand of the TCR by one amino acid [8]. We here develop a theory of the T cell response to altered peptide ligands. In section 2, we introduce the random energy model of the interaction between the TCR and the peptide-MHC complex. In section 3, we describe the process by which T cells that bind antigen are selected. In section 4, we show how experiments with altered peptide ligands may be understood with the random energy model. We discuss a critical point in the immune response probability in section 5. In section 6, we discuss correlations that may arise in forward and reverse experiments with altered peptide ligands. We conclude in section 7.

## 2 The Random Energy Model

The important molecular components of the T cell recognition event are the peptide-MHCI complex and the T cell receptor (TCR), as shown in Figure 1. Typically, the peptide ligand is on the order of 9 amino acids long. The TCR variable region is composed of 54 amino acids, grouped into 6 subdomains. The TCR sits atop the peptide-MHCI complex during recognition. Recognition of specific immunogenic peptides is due to the interaction between the subdomains of the TCR and the peptide. The majority of the amino acids in the peptide are directly recognized by 1–4 amino acids of the TCR, with typically 3 amino acids in the peptide being hot spots of the binding [9]. The entire TCR variable region interacts relatively non-specifically with the MHC complex. There is also a relatively generic interaction between the peptide and the MHC complex.

There are too many atoms within the TCR-peptide-MHCI complex and too many TCRs within an individual to treat this problem in full atomistic detail. We therefore use a type of random energy model to represent the interactions between the TCR, peptide, and MHC complex. This random energy builds

a hierarchy of correlations into Derrida’s random energy theory [10]. The immune system being a real-time example of an evolving system, the random energy approach is a natural one [11]. Our random energy model is a generalization of Kauffman’s  $NK$  model [12] to include correlations due to protein secondary structure [13,14]. The model introduced here to account for the T cell immune response contains an additional term relative to that which describes the B cell immune response [15]. In detail, our generalized  $NK$  model for the T cell response considers four different kinds of interactions: interaction within a subdomain of the TCR ( $U^{\text{sd}}$ ), interactions between subdomains of the TCR ( $U^{\text{sd-sd}}$ ), indirect interactions between the TCR and the peptide ( $U^{\text{pep-sd}}$ ), and direct binding interaction between the TCR and peptide ( $U^{\text{c}}$ ). In this model, interactions between the peptide or TCR and the MHC I have been integrated out. As is typical in statistical mechanics [16], integrating out these terms produces random interactions in the Hamiltonian, and we assume these to be roughly of the form of the other intermolecular terms in our model. In the altered peptide ligand experiments considered here, the peptides, whether original or altered, are typically expressed by the same MHC I. The first three terms of the present random energy model are identical to those used to model protein evolution [14] and the B cell antibody response [15]. The parameters within the model have been determined either by earlier work [12,13] or by structural biology [14]. The energy function of the TCR with peptide-MHC I is

$$U = \sum_{i=1}^M U_{\alpha_i}^{\text{sd}} + \sum_{i>j=1}^M U_{ij}^{\text{sd-sd}} + \sum_{i=1}^M U_i^{\text{pep-sd}} + \sum_{i=1}^{N_b} \sum_{j=1}^{N_{\text{CON}}} U_{ij}^{\text{c}}, \quad (1)$$

where  $M = 6$  is the number of TCR secondary structural subdomains,  $N_b = 3$  is the number of hot-spot amino acids that directly bind to the TCR, and  $N_{\text{CON}} = 3$  is the number of T cell amino acids contributing directly to the binding of each peptide amino acid. The subdomain energy  $U^{\text{sd}}$  is

$$U_{\alpha_i}^{\text{sd}} = \frac{1}{\sqrt{M(N - K + 1)}} \sum_{j=1}^{N-K+1} \sigma_{\alpha_i}(a_j, a_{j+1}, \dots, a_{j+K-1}), \quad (2)$$

where  $N = 9$  is the number of amino acids in a subdomain, and  $K = 4$  is the range of local interaction within a subdomain. The prefactor for this term, and the other three terms in Eq. 1, is chosen so that random sequences produce a unit variance of this term. Thus, each term in Eq. 1 contributes roughly equal weight, a priori. All subdomains belong to one of  $L = 5$  different types (*e.g.*, helices, strands, loops, turns, and others). The quenched Gaussian random number  $\sigma_{\alpha_i}$  is different for each value of its argument for a given subdomain type,  $\alpha_i$ . All  $\sigma$  values in the model are Gaussian random numbers and have zero mean and unit variance. The sigma values are different for each value

of the argument, subscript, or superscript. The variable  $\alpha_i$  defines the type of secondary structure for the  $i^{\text{th}}$  subdomain,  $1 \leq \alpha_i \leq L$ . The energy of interaction between secondary structures is

$$U_{ij}^{\text{sd-sd}} = \sqrt{\frac{2}{DM(M-1)}} \times \sum_{k=1}^D \sigma_{ij}^k(a_{j_1}^i, \dots, a_{j_{K/2}}^i; a_{j_{K/2+1}}^j, \dots, a_{j_K}^j). \quad (3)$$

We set the number of interactions between secondary structures at  $D = 2$ , as the TCR-peptide-MHCI interaction is a slightly less rough than is the antibody-antigen interaction landscape where we have used  $D = 6$  [15]. Here  $\sigma_{ij}^k$  and the interacting amino acids,  $j_1, \dots, j_K$ , are selected at random for each interaction  $(i, j, k)$ . The indirect interaction energy between the peptide and the TCR is given by

$$U_i^{\text{pep-sd}} = \sqrt{\frac{1}{DM}} \sum_{k=1}^D \sigma_i^k(a_{j_1}^{\text{pep}}, \dots, a_{j_{K/2}}^{\text{pep}}; a_{j_{K/2+1}}^i, \dots, a_{j_K}^i). \quad (4)$$

Here  $\sigma_i^k$  and the interacting amino acids,  $j_1, \dots, j_K$ , are selected at random in the peptide and TCR subdomain for each interaction  $(i, k)$ . The chemical binding energy of each TCR amino acid to the peptide is given by

$$U_{ij}^c = \frac{1}{\sqrt{N_b N_{\text{CON}}}} \sigma_{ij}(a_{j_1}^{\text{pep}}, a_{j_2}). \quad (5)$$

The contributing amino acids,  $j_1, j_2$ , and the unit-normal weight of the binding,  $\sigma_{ij}$ , are chosen at random for each interaction  $(i, j)$ , with  $N_b$  possible values for  $j_1$ , and  $NM$  possible values for  $j_2$ .

Although there are 20 different naturally occurring amino acids, there are only roughly five distinct classes. Mutations that change an amino acid to another within the same class are termed conservative, whereas mutations that change the class of the amino acid are termed non-conservative. This distinction is significant because non-conservative mutations change the energy landscape more dramatically than do conservative mutations. Non-conservative mutations lead to a factor of  $2.34 \approx (1 + 1/2^2)^{1/2} / (1/2)$  greater energy change than do conservative mutations, on average as estimated from statistically determined energy values from the protein sequence alignment matrix (PAM) [17]. To consider all 20 amino acids within the random energy model, Eq. 1, and to consider the differing effects of conservative and non-conservative mutations, we set the random  $\sigma$  for amino acid  $i$  that belongs to group  $j$  as  $\sigma = w_j + w_i/2$ ,

where the  $w$  are Gaussian random numbers with zero average and unit standard deviation. There are 5 groups, with 8 amino acids in the neutral and polar plus cystein group, 2 amino acids in the negative and polar group, 3 amino acids in the positive and polar group, 4 amino acids in the nonpolar without ring group, and 3 amino acids in the nonpolar with ring group. The results are not greatly sensitive to the precise groupings of the amino acids.

The naive TCR repertoire is generated randomly from gene fragments. This is accomplished by constructing the TCRs from subdomain pools. Fragments for each of the  $L$  subdomain types are chosen randomly from 5 of the 100 lowest energy subdomain sequences. This diversity mimics the known TCR diversity,  $(5 \times L)^M \approx 10^8$ . There have been recent suggestions that the possible diversity of a given individual's TCR repertoire is  $\approx 10^{11}$ , with the actual diversity expressed at any point in time being  $\approx 10^8$  [18]. These numbers, which are very much in line with the numbers for human antibodies, would imply  $L = 13$ . The results for the present study are not greatly sensitive to whether  $L = 5$  or  $L = 13$ .

The binding constants between the peptide-MHCI ligand and the TCR are calibrated by fixing the worst and geometric mean of the binding constants evolved during a primary response to be  $3 \times 10^5$  l/mol and  $3 \times 10^6$  l/mol, respectively, where the binding constant is related to the energy by

$$k = e^{a-bU} . \tag{6}$$

That is, fixing the worst and geometric mean of the binding constants to these values determines the values of  $a$  and  $b$  for each instance of the random parameters with in the generalized  $NK$  model. This approach leads to the best binding constant being on average  $3 \times 10^7$  l/mol. These binding constants are taken from experiment [19] and are slightly smaller than those for antibodies. Whenever the peptide substrate is changed, the constants  $a$  and  $b$  in Eq. 6 are reevaluated by comparison to the existing naive TCR repertoire. All terms from Eq. 1 are significant, because which of the TCRs from the repertoire best bind depends on the identity of the peptide.

### 3 The T Cell Maturation Process

The T-cell-mediated response is driven by cycles of concentration expansion and selection for better binding constants. Selection processes are ubiquitous in nature [20], although the exact mechanism of the T cell expansion during the primary immune response remains elusive. It is clear that the expansion of the T cells is non-linear [3]. It also seems that, in most cases, there is

competition among the T cells for the presented antigen [7,21]. Since the T cells do not mutate during the primary response, our model of the primary response dynamics to be detailed below can be viewed as one particular description of the non-linear expansion of the naive T cell repertoire. The primary response increases the concentration of selected TCRs by 1000 fold over 10 days, with a rough T cell doubling time of one day. The diversity of the memory sequences is 0.5% of that of the naive repertoire [2]. The secondary response increases the concentration of the selected sequences by 10 fold over a few days. For humans, there are roughly  $2.5 \times 10^7$  distinct T cell sequences at a copy number of  $2.4 \times 10^4$  in the naive repertoire and roughly  $1.5 \times 10^5$  sequences at a copy number of  $2 \times 10^6$  in the memory repertoire [2]. Typical best and worst binding constants of the memory repertoire are  $10^7$  l/mol and  $10^5$  l/mol, respectively [19].

We implement a selection model of the T cell immune system maturation. Specifically, 10 rounds of selection are performed during the primary response, with the top  $x = 58\%$  of the sequences chosen at each round. That is, the probability of picking one of the sequences for the next round is

$$P_{\text{select}} = \begin{cases} \frac{1}{0.58N_{\text{size}}}, & \text{for } U \leq U_* \\ 0, & \text{for } U > U_* \end{cases} \quad (7)$$

where  $U_*$  is the energy for which 58% of the sequences lie below. This equation is employed  $N_{\text{size}}$  times, where  $N_{\text{size}}$  is the diversity of the T cell repertoire, *i.e.* the number of distinct T cell present within the immune system, to select randomly the  $N_{\text{size}}$  sequences for the next round. This procedure mimics the concentration expansion factor of  $10^3 \approx 2^{10}$  in the primary response and leads to 0.5% diversity of the memory repertoire, because  $0.58^{10} \approx 0.5\%$  and 10 days of doubling leads to a concentration expansion of  $2^{10} = 1024$ .

As discussed in more detail in section 4, the quality of the primary immune response is often measured experimentally by an *in vitro* or *ex vivo* assay. For an *in vivo* secondary response, we calculate the average binding constants of the memory and naive responses, and whichever is larger determines whether the response will be from the memory or naive repertoires. In fact, the memory binding constant is multiplied by a factor of 100, as memory T cells are present at higher concentrations and more broadly present in the tissue than are naive T cells. If the memory cells are used in the secondary *in vivo* response, the top  $x = 58\%$  of the sequences are chosen, and 3 rounds of selection are performed [3,4]. This mimics the concentration factor of  $10 \approx 2^3$  during the secondary memory response. Conversely, if the naive cells are used in the secondary *in vivo* response, the dynamics is identical to that of the primary response. For an *in vitro* secondary response, in which memory T cells are extracted and stimulated in an *in vitro* experiment, 3 rounds of selection are performed,

starting with exclusively memory sequences.

Implementation of our theory proceeds by computational simulation of the generalized  $NK$  model. First, the peptide and the altered peptide ligands are created. Then, the random terms such as the secondary structural types of the subdomains, the  $\sigma$  values, the binding sites, and the interaction sites of the generalized  $NK$  model are determined. Then the fraction and identity of the T cell repertoire that responds well to the peptide ligand is identified. Typically, 1 in  $10^5$  T cells responds well to any particular ligand, and one thus expects on the order of  $10^8/10^5 = 1000$  T cells to participate in the naive response. Then the values of the constants  $a$  and  $b$  in Eq. 6 are calculated. The primary response of 10 rounds of selection is then carried out. Finally, the secondary response, either 10 rounds from the naive pool or 3 rounds from the memory pool, depending on the relative binding constants for the altered peptide is carried out.

#### 4 Experiments with Altered Peptide Ligands

A fundamental way to measure the correlation between immune responses to related antigens is to use altered peptide ligands (APLs). In such experiments, an immune response is first generated to the original peptide. The peptide antigen is then changed, typically either conservatively or non-conservatively and only at one amino acid position [22]. The immune response to this altered peptide antigen is then measured. Intuitively, one expects that if the peptide antigen is altered only slightly, the immune response to the APL will be relatively high, whereas if the peptide is altered significantly, the immune response to the APL will be rather low.

Specific lysis is a measure of the probability that an activated T cell will recognize an antigen presenting cell that is expressing a particular peptide-MHCI complex. This quantity is measured as a function of the effector to target ratio,  $E_0/T_0$ , the ratio of the number of T cells to the number of antigen presenting cells. Each T cell typically expresses on the order of  $10^5$  identical TCRs, and each antigen presenting cell typically expresses on the order of  $2 \times 10^4$  peptide-MHCI complexes [19]. In typical experiments, the specific lysis is measured over a 4 hour time period [23]. Although T cells can each kill many targets *in vivo*, the experimental specific lysis assay requires the number of T cells to be greater than the number of targets for detectable killing. Lysis is a statistical event, being on average roughly proportional to the probability of a T cell binding the target cell. To calculate the specific lysis curve, we calculate the amount of the target cells that are bound by all T cells. We do this by considering the equilibrium between the effector T cells

and the target antigen presenting cells:

$$E_i + T \rightleftharpoons E_i T, \quad K_i . \quad (8)$$

This equation implies  $[E_i T]/([E_i][T]) = K_i$ . Introducing the amount of antigen presenting cells that are bound by T cell  $i$ ,  $\xi_i$ , and noting that the effector concentration is typically higher than the concentration of antigen presenting cells, we find

$$\xi_i = K_i E_i^0 (T_0 - \sum_i \xi_i) . \quad (9)$$

Summing over all T cells, we find for the total amount of antigen presenting cells bound by any T cell:

$$L = \frac{\sum_i K_i E_i^0}{1 + \sum_i K_i E_i^0} . \quad (10)$$

where  $L = \sum_i \xi_i/T_0$  is the specific lysis. Writing this in the form

$$L = \frac{z E_0/T_0}{1 + z E_0/T_0} , \quad (11)$$

we find  $z = T_0 \sum_i K_i E_i^0/E_0 = T_0 \langle K \rangle$ . Thus, the competitive binding process for the antigen presenting cells can be viewed as a Langmuir adsorption isotherm of the T cells onto the antigen presenting cells.

The binding constant  $K_i$  is that between the two cells. Assuming that the free energies of binding for each of the TCR/peptide-MHCI interactions are approximately additive, we find  $K_i = 10^5 \times 2 \times 10^4 k_i$ , where  $k_i$  is the molecular binding constant between TCR  $i$  and the peptide-MHCI complex. Typical values of the target cell concentration are  $2 \times 10^3$  target cells in 200  $\mu\text{l}$  of solution, or  $T_0 = 1.66 \times 10^{-17}\text{M}$  [23]. We, thus, find

$$z = \frac{\langle k \rangle}{3 \times 10^7} . \quad (12)$$

Interestingly, the maximum value of the binding constant in Eq. 6 is of the same order of magnitude as the denominator in Eq. 12. For convenience, we have chosen them to be identical. Adding in some cooperativity in the binding, *i.e.* assuming that the free energies of binding for each of the TCR/peptide-MHCI interactions are not entirely additive, will only change details such as the denominator in Eq. 12.

At infinite dilution of the T cells, we find that the average number of antigen presenting cells that are lysed by one T cell is  $LT_0/E_0 = z$ . The quantity  $z$  is, therefore, the average clearance probability of one T cell. Since the T cell typically can lyse no more than one target cell in specific lysis assays, we modify the definition of the clearance probability as

$$z = \frac{1}{N_{\text{size}}} \sum_{i=1}^{N_{\text{size}}} \min(1, k_i/3 \times 10^7) . \quad (13)$$

This equation is implemented by introducing a lower cutoff in the energy according to  $3 \times 10^7 = \exp(a - bU_{\text{min}})$ .

The immune response probability is a measure of the probability that the clearance probability is greater than 50%. In other words, the immune response probability is the average of  $H(L - 1/2)$ , where  $H(x) = 0, x < 0$  and  $H(x) = 1, x > 0$ . Both the specific lysis and the immune response probability are averaged over many instances of the random energy model, typically  $10^4$ .

Both specific lysis and immune response probability can be measured experimentally either *in vitro* or *ex vivo*. Typically these responses are measured after the primary response to the original peptide ligand and before a true secondary response to the altered peptide ligand. Experimentally, the *ex vivo* response is measured by preparing mice, immunizing with the virus, and after 8–10 days removing the spleen of the mouse. The T cells from the spleen are then challenged with antigen presenting cells expressing the specific altered peptide ligand. The spleen in this case contains both memory and naive T cells. For the *ex vivo* APL response, we use  $N_{\text{size}}/2$  distinct memory cells and  $N_{\text{size}}$  distinct naive cells, where  $N_{\text{size}}$  is the diversity of the naive T cell repertoire, to calculate the observables [2]. Experimentally, the *in vitro* response is measured by removing the spleen of the mouse, immunizing the spleen cells with the virus, and after 8-10 days challenging those spleen cells with antigen presenting cells expressing the specific altered peptide ligand. The spleen in this case contains predominantly memory cells. For the *in vitro* APL response, we use exclusively  $N_{\text{size}}$  memory cells to calculate the observables.

We use this theory to analyze the correlations in the immune response that are measured in altered peptide ligand experiments. The non-linear susceptibility of the random energy model to structural changes allows us to capture the correlations in the immune response to altered peptide antigens. An extensive set of quantitative experiments on altered peptide ligands has been carried out on the mouse model viral disease lymphocytic choriomeningitis virus (LCMV). Due to the particularly strong immunogenicity of LCMV, the memory T cell population is comprised essentially exclusively of T cells from the primary LCMV response, in contrast to the more typical case where 1-10% of the memory T cell population is specific for a particular disease [24]. Shown in

Figure 2 is a comparison between the measured and calculated *ex vivo* and *in vitro* responses to altered peptide ligands with a single non-conservative mutation. Experiments have been carried out with conservative mutations as well, and shown in Figure 3 is a comparison between the measured and calculated *ex vivo* and *in vitro* responses to altered peptide ligands with a single conservative mutation.

The *in vitro* response is always greater than the *ex vivo*, because a purely memory response is better than a naive response for these peptides altered by one amino acid. The responses are slightly superior for the conservative mutations than for the non-conservative mutations, because in the conservative case the altered peptide is more similar to the original peptide upon which the memory sequences were evolved.

Immune response probabilities have not been widely measured. In a classic study, Klenerman and Zinkernagel found that 1 out of 7 non-conservatively altered peptides produced a response to LCMV [22]. This data point is shown in Figure 4. Also shown are the *ex vivo* and *in vitro* immune response probabilities to altered peptide ligands with a single non-conservative mutation. Shown in Figure 5 are the *ex vivo* and *in vitro* immune response probabilities to altered peptide ligands with a single conservative mutation.

The *in vitro* response remains superior to the *ex vivo* response, as the peptides with a single amino acid mutation are best recognized by the memory sequences. In addition, the conservative response is stronger than the non-conservative response, because the conservatively mutated peptides are more similar to the native target of the memory sequences than are the non-conservatively mutated peptides.

## 5 A Critical Point in the Immune Response Probability

It can be seen that larger repertoire sizes lead to a sharpening of the immune response probability curve. In fact, there is a critical point in our model which occurs at  $E_0/T_0 = 4.6$  for the *in vitro* and  $E_0/T_0 = 16$  for the *ex vivo* case. The critical immune response probability lies in the range 0.14–0.23. The critical value of  $E_0/T_0$  is shifted to a higher value for the *ex vivo* case because the average energies are not as favorable in this case. Randomness in the ensemble, due to the energy fluctuations, causes the immune response probability in the infinite repertoire limit to be a smooth curve, rather than a step function. Such randomness would correspond, for example, to the variability in an individual’s response to a variety of disease strains or the variability in the response of a population of individuals to a specific disease strain. In our model, there is an additional source of randomness for a finite repertoire size, the inexact

evaluation of the constants  $a$  and  $b$  in Eq. 6. Assuming that the variation in  $a$  is more significant and is Gaussian, we can roughly say  $z = \exp(a + \alpha\sigma - bU)$ , where  $\sigma$  is a Gaussian with unit variance and zero mean,  $\alpha = O(1/\sqrt{N_{\text{size}}})$  is the rough size in the error of the calculation of  $a$ , and  $U$  is random with a certain probability distribution. We calculate the contribution of the randomness in  $a$  to the immune response probability,  $F$ , as

$$\begin{aligned}
\frac{\partial F}{\partial \alpha} &= \left\langle \frac{\partial H}{\partial L} \frac{\partial L}{\partial \alpha} \right\rangle \\
&= \left\langle \delta(L - 1/2) \frac{\partial L}{\partial z} \frac{\partial z}{\partial \alpha} \right\rangle \\
&= \frac{1}{4} \langle \sigma | L = 1/2 \rangle \\
&= \frac{1}{4} \int d\sigma P(\sigma) \sigma \int du P(u) \delta(L - 1/2) \\
&= \frac{1}{b} \int d\sigma P(\sigma) \sigma P(u^*) \Big|_{x \exp(a + \alpha\sigma - bu^*) = 1}
\end{aligned} \tag{14}$$

Assuming that the randomness in the energy is also Gaussian, we find

$$\begin{aligned}
F &= F_0 - \frac{\alpha^2}{2b^2} x^{(-a+b\langle u \rangle)/(b^2\chi)} e^{-[(a-b\langle u \rangle)^2 + \ln^2 x]/(2b^2\chi)} \\
&\quad \times \frac{a - b\langle u \rangle + \ln x}{\chi(2\pi\chi)^{1/2}}
\end{aligned} \tag{15}$$

where  $\chi = \langle (u - \langle u \rangle)^2 \rangle$ . The fixed point occurs for  $x^* = \exp(-a + b\langle u \rangle)$  and  $F^* = 1/2$ . The deviation of the immune response probability from the infinite repertoire size limit is  $O(\alpha^2) = O(1/N_{\text{size}})$ . The shape of this curve is very similar to that seen in Figures 4 and 5. If we make a more detailed analysis that takes into account the negative asymmetry of the probability distribution for  $\ln z$ , which is due to the cutoff in Eq. (13), we find that  $F^*$  is lowered from  $1/2$ . The *ex vivo* probability distribution for  $\ln z$  is more symmetric than is the *in vitro* probability distribution, and so the *ex vivo* fixed point should be higher than the *in vitro* fixed point. In addition, the conservative probability distribution for  $\ln z$  has a smaller negative tail than does the non-conservative distribution, and so the conservative fixed point should be higher than the non-conservative fixed point. These predictions are in agreement with the observations in Figures 4 and 5.

## 6 Correlation in Forward and Reverse APL Experiments

Using our random energy model, it is possible to examine how correlations in the forward altered peptide ligand experiment give rise to altered correlations

in the reverse altered peptide ligand experiment. For example in Ref. [22], one set of experiments was performed with LCMV wild-type as the original peptide and LCMV-8.7 as the altered peptide ligand, and another set of experiments was performed with LCMV-8.7 as the original peptide and LCMV wild type as the altered peptide ligand. In Figure 6, we show these data as well as a representative set of curves from our theory.

A more systematic way to study such forward and reverse experiments is to look at the correlation between a response in the forward original peptide ligand (OPL)  $\rightarrow$  APL experiment and the reverse APL  $\rightarrow$  OPL experiment. We introduce the correlation matrix

$$C = \begin{pmatrix} \langle z_A z_B \rangle & \langle z_A(1 - z_B) \rangle \\ \langle (1 - z_A)z_B \rangle & \langle (1 - z_A)(1 - z_B) \rangle \end{pmatrix}. \quad (16)$$

Here  $z_A$  is the *in vitro* clearance probability of the APL in the forward experiment where the memory sequences were evolved against the OPL, and  $z_B$  is the *in vitro* clearance probability of the OPL in the reverse experiment, where the memory sequences were evolved against the APL. The averages are taken over instances of the random energy model. Although the average response is the same for the forward and reverse experiments,  $\langle z_A \rangle = \langle z_B \rangle$ , there may be a correlation between the two responses. To specify the notation, we note that the probability of a forward response is given by  $P(A) = \langle z_A \rangle$  and that of a reverse response by  $P(B) = \langle z_B \rangle$ . The probability of both a forward and reverse response is given by  $P(A, B) = \langle z_A z_B \rangle = C_{11}$ . The conditional probability that the reverse experiment is successful, given that the forward experiment is successful, is

$$P(B|A) = \frac{P(A, B)}{P(A)} = \frac{P(A, B)}{P(B)} = \frac{C_{11}}{\langle z_A \rangle}. \quad (17)$$

From our model, we find  $\langle z_A \rangle = 0.113$  and  $C_{11} = 0.01651$ , and thus  $P(B|A) = 0.146$ . These values are not greatly sensitive to the repertoire size. The cross correlation is given by  $(\Delta C)^2 = C_{11} - P(A)P(B) = 0.003797$ . The cross correlation can alternatively be expressed as

$$\frac{P(B|A)}{P(A)} = 1 + \left( \frac{\Delta C}{P(A)} \right)^2. \quad (18)$$

If there were no correlation between the two experiments, we would find  $P(B|A)/P(A) = 1$ . If there were complete correlation between the experiments,  $P(B|A)/P(A) = 1/P(A) = 8.87$ . In fact, we find in our model that  $P(B|A)/P(A) = 1.30$ , showing a modest amount of correlation between the

OPL  $\rightarrow$  APL and APL  $\rightarrow$  OPL experiments. Experimental measurements of this predicted correlation would be very interesting.

## 7 Summary

The random energy model of the T cell immune system presented here allows an investigation of the sequence-level evolution that occurs within the T cell repertoire. This is remarkable, given the complexity underlying the immune response. Correlations in the immune response to mutated antigens are captured by the non-linear susceptibility of the underlying random energy model to structural changes. Specific lysis curves for the model virus LCMV are well predicted by the theory. The immune response probability is shown to vary in a systematic fashion with the effector to target ratio, and more experimental measurements of this quantity are needed.

The effective design of vaccines for viral diseases requires some estimation of the likely escape mechanisms of the virus. For example, for rapidly mutating strains, a highly-diverse, multicomponent vaccine may be necessary to halt progression and transmission of the virus. Conversely, for slowly evolving strains, diversity within the vaccine may simply dilute the conference of protective immunity. The approach taken here allows investigation and determination of the fundamental qualitative and quantitative features that govern the interaction between an effective multicomponent vaccine and the variability of the virus. The theory complements and may provide some guidance to the long and difficult process of experimental multicomponent vaccine development against escaping viral diseases.

## Acknowledgments

It is a pleasure to acknowledge stimulating discussions with Michael A. Barry. This research was supported by the National Institutes of Health and the National Science Foundation.

## References

- [1] A. S. Perelson, G. Weisbuch, Immunology for physicists, Rev. Mod. Phys. 69 (1997) 1219–1267.

- [2] T. P. Arstila, A. Casrouge, V. Baron, J. Even, J. Kanellopoulos, P. Kourilsky, Direct estimate of the human  $\alpha\beta$  T cell receptor diversity, *Science* 286 (1999) 958–961.
- [3] J. N. Blattman, D. J. D. Sourdive, K. Murali-Krishna, R. Ahmed, J. D. Altman, Evolution of the T cell repertoire during primary, memory, and recall responses to viral infection, *J. Immunol.* 165 (2000) 6081–6090, Note the non-linear expansion of the different T cells between the naive and primary repertoires in Figure 1.
- [4] D. J. D. Sourdive, K. Murali-Krishna, J. D. Altman, A. J. Zajac, J. K. Whitmire, C. Pannetier, P. Kourilsky, B. Evavold, A. Sette, R. Ahmed, Conserved T cell receptor repertoire in primary and memory CD8 T cell responses to an acute viral infection, *J. Exp. Med.* 188 (1998) 71–82.
- [5] K. H. Lee, A. D. Holdorf, M. L. Dustin, A. C. Chan, P. M. Allen, A. S. Shaw, T cell receptor signaling precedes immunological synapse formation, *Science* 295 (2002) 1539–1542.
- [6] K. H. Lee, A. R. Dinnner, C. Tu, G. Campi, S. Raychaudhuri, R. Varma, T. N. Sims, W. R. Burack, H. Wu, O. Kanagaw, M. Markiewicz, P. M. Allen, M. L. Dustin, A. K. Chakraborty, A. S. Shaw, The immunological synapse balances T cell receptor signaling and degradation, *Science* 302 (2003) 1218–1222.
- [7] R. M. Kedl, J. W. Kappler, P. Marrack, Epitope dominance, competition and T cell affinity maturation, *Curr. Opin. Immunol.* 15 (2003) 120–127.
- [8] J. Sloan-Lancaster, P. M. Allen, Altered peptide ligand-induced partial T cell activation: Molecular mechanisms and role in T cell biology, *Annu. Rev. Immunol.* 14 (1996) 1–27.
- [9] K. C. Garcia, M. Degano, L. R. Pease, M. Huang, P. A. Peterson, L. Teyton, I. A. Wilson, Structural basis of plasticity in T cell receptor recognition of a self peptide-MHC antigen, *Science* 279 (1998) 1166–1172.
- [10] B. Derrida, Random energy model—Limit of a family of disordered models, *Phys. Rev. Lett.* 45 (1980) 79–82.
- [11] B. Derrida, L. Peliti, Evolution in a flat fitness landscape, *Bull. Math. Biol.* 53 (1991) 355–382.
- [12] S. Kauffman, S. Levin, Towards a general-theory of adaptive walks on rugged landscapes, *J. Theor. Biol.* 128 (1987) 11–45.
- [13] A. S. Perelson, C. A. Macken, Protein evolution on partially correlated landscapes, *Proc. Natl. Acad. Sci. USA* 92 (1995) 9657–9661.
- [14] L. D. Bogarad, M. W. Deem, A hierarchical approach to protein molecular evolution, *Proc. Natl. Acad. Sci. USA* 96 (1999) 2591–2595.
- [15] M. W. Deem, H.-Y. Lee, Sequence space localization in the immune system response to vaccination and disease, *Phys. Rev. Lett.* 91 (2003) 068101.

- [16] D. Chandler, Introduction to Modern Statistical Mechanics, Oxford University Press, New York, 1987.
- [17] M. O. Dayhoff, R. M. Schwartz, B. C. Orcutt, A model of evolutionary change in proteins, in: Atlas of Protein Sequence and Structure, Vol. 5, National Biomedical Research Foundation, 1978, pp. 345–352.
- [18] C. Kesmir, J. A. M. Borghans, R. J. de Boer, Diversity of human  $\alpha\beta$  t cell receptors, Science 288 (2000) 1135.
- [19] B. A. Schodin, T. J. Tsomides, D. M. Kranz, Correlation between the number of T cell receptors required for T cell activation and TCR-ligand affinity, Immunity 5 (1996) 137–146.
- [20] B. Drossel, Biological evolution and statistical physics, Adv. Phys. 50 (2001) 209–295.
- [21] It is not clear whether this competition occurs during each and every round of T cell division during the primary response.
- [22] P. Klenerman, R. M. Zinkernagel, Original antigenic sin impairs cytotoxic T lymphocyte responses to viruses bearing variant epitopes, Nature 394 (1998) 482–485.
- [23] M. F. Bachmann, D. E. Speiser, P. S. Ohashi, Functional maturation of an antiviral cytotoxic T-cell response, J. Virol. 71 (1997) 5764–5768.
- [24] R. A. K. Singh, J. R. Rodgers, M. A. Barry, The role of T cell antagonism and original antigenic sin in genetic immunization, J. Immunol. 169 (2002) 6779–6786.
- [25] D. N. Garboczi, P. Ghosh, U. Utz, Q. R. Fan, W. E. Biddison, D. C. Wiley, Structure of the complex between human T-cell receptor, viral peptide and HLA–A2, Nature 384 (1996) 134–141.
- [26] M. F. Bachmann, D. E. Speiser, A. Zakarian, P. S. Ohashi, Inhibition of TCR triggering by a spectrum of altered peptide ligands suggests the mechanism for TCR antagonism, Eur. J. Immunol. 28 (1998) 3110–3119.
- [27] S. Martin, H. Kohler, H. U. Weltzien, C. Leipner, Selective activation of CD8 T cell effector functions by epitope variants of lymphocytic choriomeningitis virus glycoprotein, J. Immunol. 157 (1996) 2358–2365.

## Figures

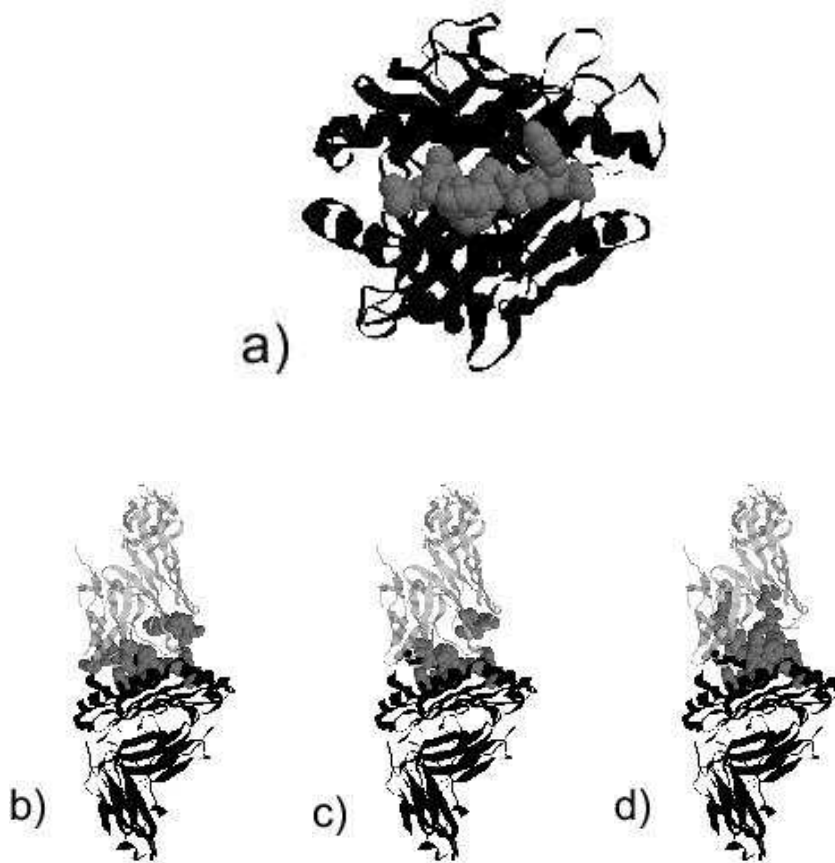


Fig. 1. Figure of the interaction between the TCR and the peptide-MHCI complex. The TCR consists of two domains,  $\alpha$  and  $\beta$ , each of which contains three complementary determining regions (CDRs) that interact with the peptide-MHCI complex. The MHC I complex consists of two domains,  $\alpha$  and  $\beta$ , and the  $\alpha$  domain is comprised of two halves,  $\alpha_1$  and  $\alpha_2$ . a) Top view of the peptide-MHCI complex. The peptide (gray) sits like a “hotdog in a bun” in the  $\alpha_1$  and  $\alpha_2$  domains of the MHC I complex (black). b) Side view of CDR 1 (gray) from TCR domain  $\alpha$  interacting with the first few amino acids of the peptide and the MHC I and of CDR 1 (gray) from TCR domain  $\beta$  interacting with the last few amino acids of the peptide and the MHC I. The TCR (light gray) sits on top of the peptide-MHCI complex. The peptide sits between the TCR and MHC I complex. c) CDR 2 (gray) from TCR domain  $\alpha$  interacts with the first few amino acids of the peptide and the MHC I, and CDR 2 (gray) from TCR domain  $\beta$  interacts with the last few amino acids of the peptide and the MHC I. d) CDR 3 (gray) from both TCR domains interacts with the middle few amino acids of the peptide. Atomistic details of this interaction are from an X-ray crystal structure ([25], <http://www.rcsb.org/pdb/>, accession number 1AO7). The interactions between the peptide and the TCR are represented by the last two terms of Eq. 1. The TCR itself must fold, and these terms are represented by the first two terms of Eq. 1. The interactions between the TCR and the MHC I complex have been integrated out in the model.

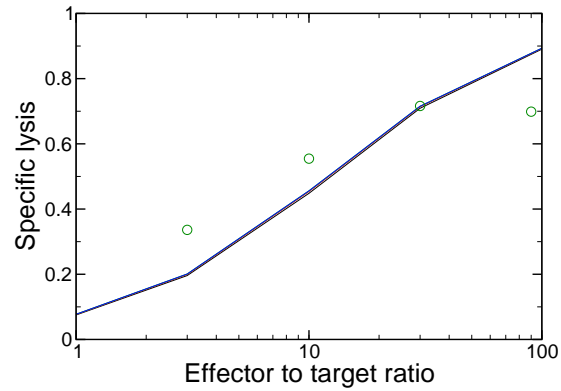
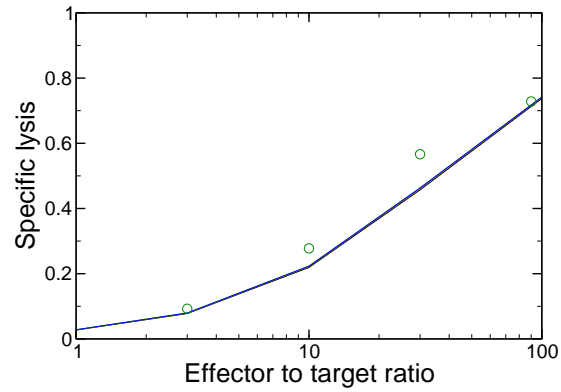


Fig. 2. Specific lysis as a function of effector to target ratio for repertoire sizes in the range  $10^3$  to  $10^6$  for non-conservatively altered peptide ligands. The theoretical curves overlap for all repertoire sizes. Results are for *ex vivo* (upper) and *in vitro* (lower). Experimental data (circles) are from the LCMV mouse models of [23] (*ex vivo*) and [26] (*in vitro*).

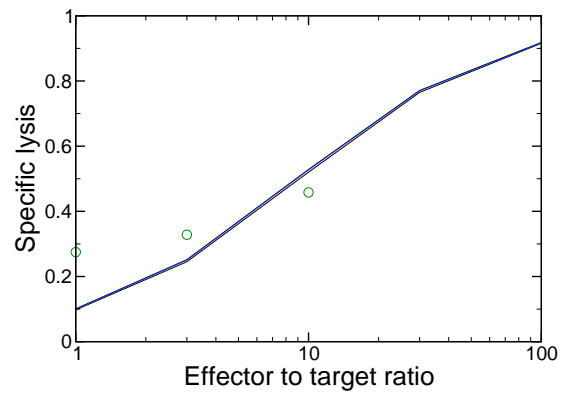
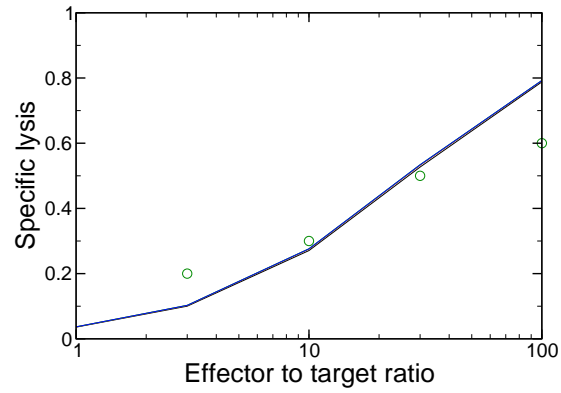


Fig. 3. Specific lysis as a function of effector to target ratio for repertoire sizes in the range  $10^3$  to  $10^6$  for conservatively altered peptide ligands. Results are for *ex vivo* (upper) and *in vitro* (lower). Experimental data (circles) are from the LCMV mouse models of [22] (*ex vivo*) and [27] (*in vitro*).

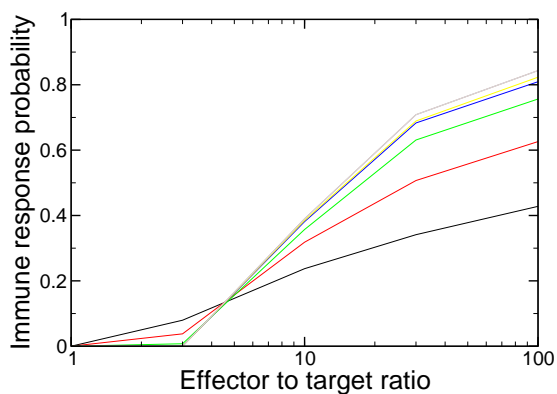
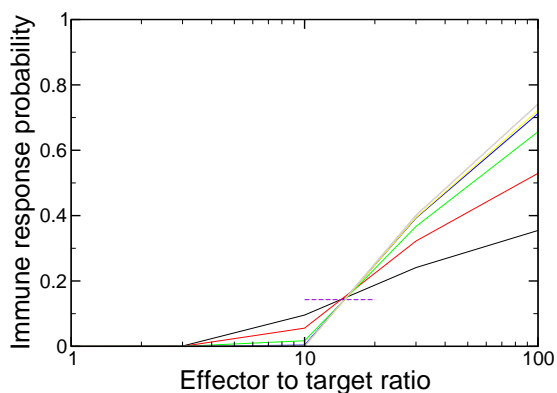


Fig. 4. Immune response probability as a function of effector to target ratio for repertoire sizes of  $10^3$ ,  $3 \times 10^3$ ,  $10^4$ ,  $3 \times 10^4$ ,  $10^5$ , and  $3 \times 10^5$  for non-conservatively altered peptide ligands. Larger repertoire sizes lead to a greater slope at the inflection point of the curve. Results are for *ex vivo* (upper) and *in vitro* (lower). Experimental datum (horizontal dashed line) is taken from the LCMV mouse model of [22] (live mouse, *in vivo*).

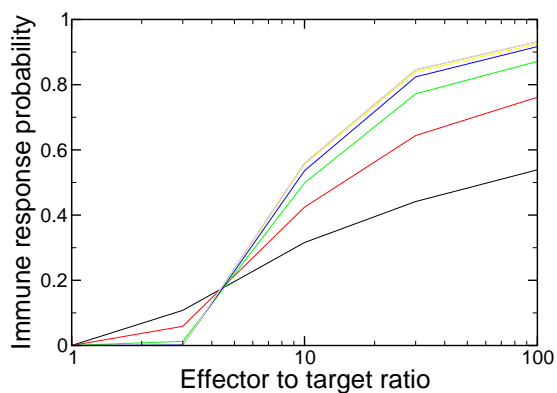
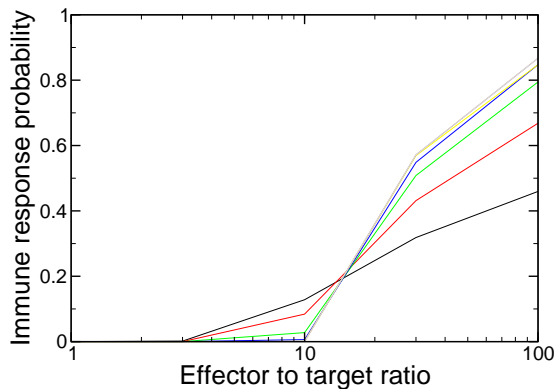


Fig. 5. Immune response probability as a function of effector to target ratio for conservatively altered peptide ligands. Repertoire sizes as in Figure 4. Results are for *ex vivo* (upper) and *in vitro* (lower).

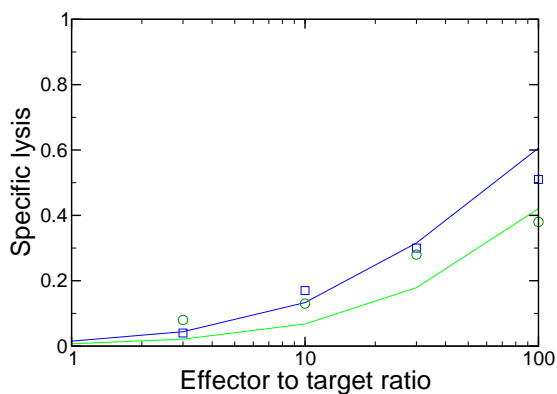


Fig. 6. Representative specific lysis curves for a forward and backward altered peptide ligand experiment. Data from experiments with LCMV-WE original ligand and LCMV-8.7 altered peptide ligand (circles) and LCMV-8.7 original ligand and LCMV-WE altered peptide ligand (squares) from the *in vitro* LCMV mouse model of [22].